Cationic β-Lactoglobulin Nanoparticles as a Bioavailability Enhancer: Protein Characterization and Particle Formation

ARTICLE *in* BIOMACROMOLECULES · JUNE 2013

Impact Factor: 5.75 · DOI: 10.1021/bm4006886 · Source: PubMed

5 AUTHORS, INCLUDING:

Zi Teng
University of Maryland, College Park
28 PUBLICATIONS **398** CITATIONS
SEE PROFILE

Yangchao Luo
University of Connecticut
53 PUBLICATIONS **937** CITATIONS
SEE PROFILE

Boce Zhang
University of Maryland, College Park
22 PUBLICATIONS **457** CITATIONS
SEE PROFILE

Qin Wang
University of Maryland, College Park
71 PUBLICATIONS **911** CITATIONS
SEE PROFILE

Article

pubs.acs.org/Biomac

Cationic β-Lactoglobulin Nanoparticles as a Bioavailability Enhancer: Protein Characterization and Particle Formation

Zi Teng,[†] Ying Li,[‡] Yangchao Luo,[†] Boce Zhang,[†] and Qin Wang*[,†]

[†]Department of Nutrition and Food Science, University of Maryland, 0112 Skinner Building, College Park, Maryland 20742, United States

[‡]College of Light Industry and Food Science, South China University of Technology, Tianhe District, Guangzhou, 510640, People's Republic of China

Supporting Information

ABSTRACT: Cationic β-lactoglobulin (CBLG) was developed as a bioavailability enhancer for poorly absorbed bioactives. At most 11 anionic amino acid residues of β-lactoglobulin (BLG) were substituted by ethylenediamine (EDA), resulting in a highly positive surface charge (zeta potential up to 39 mV at pH 7.0) and significantly increased surface hydrophobicity. These changes conferred CBLG with desirable water solubility and improved mucoadhesion by at most 252%, according to quartz crystal microbalance (QCM) study. Furthermore, CBLG inherited the unique resistance to gastric digestion from BLG, while the digestion under simulated intestinal condition was significantly improved. The latter was possibly due to the formation of aspartic acid-EDA conjugates, together with the randomization of protein conformation related with decreased percentage of β-sheet. Compared to BLG, CBLG formed smaller (75−94 nm), more uniform nanoparticles by the acetone-desolvation method. These merits made CBLG a useful material that provides desirable solubility, controlled release, and enhanced absorption to nutraceuticals or drugs.

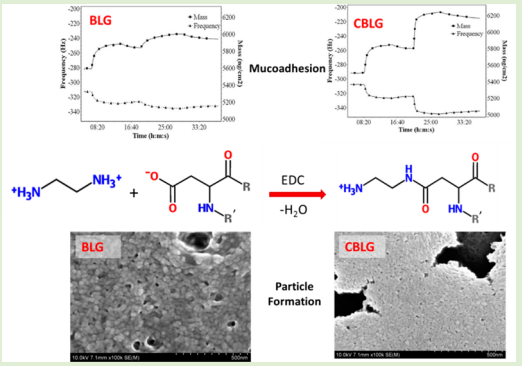

INTRODUCTION

In the past few decades, nanoencapsulation has been recognized as an effective approach to enhanced bioavailability of poorly absorbed nutraceuticals and drugs.[1] For orally administered compounds, successful absorption requires an appropriate encapsulant with a number of features. These include sufficient loading capacity, high dispersion stability,[1] resistance to gastric digestion,[2] satisfactory mucoadhesion,[3] increased cellular uptake,[4] and prolonged circulation time.[5] The last property could be obtained through the fabrication of nanoscaled vehicles,[6] while the rest of them could be conferred to the encapsulants by carefully tuning their surface properties, among which charge and hydrophobicity play critical roles.[7]

Cationic polymers, such as chitosan,[8,9] lactoferrin[10,11] and polylysine,[12] showed satisfactory mucoadhesive properties as well as cellular internalization efficacy. Such improvement was attributed to an enhanced electrostatic interaction with the anionic glycoproteins and glycolipids, which were abundant on the small intestinal wall or cell membrane.[13,14] In addition, peptides that possessed both positive net charge and a hydrophobic exterior (known as cell penetrating peptides or CPPs) were synthesized.[15−17] The conjugation of CPPs to drug-loaded nanoribbions,[18] nanoparticles,[19] or nanocomplexes[20] resulted in elevated cellular uptake. In spite of the above-mentioned merits, there exist several drawbacks in these cationic encapsulants, which impeded the effective delivery of orally ingested bioactives. For example, chitosan-based nanoparticles are insoluble at neutral to basic pH, which might compromise their claimed advantages in mucoadhesion and cellular uptake in vivo. Such insolubility may also confine their application to acidic food systems. Cationic peptide- or protein-based delivery systems are soluble in water, but their susceptibility to peptic digestion in the stomach may result in the loss of protection before absorption occurs.[21] These disadvantages necessitate the development of a water-soluble, pepsin-resistant, cationic delivery system.

β-Lactoglobulin (BLG), a 162-residue globular protein, makes up approximately 60% of bovine whey protein.[22] Owing to its high water solubility and unique structure, BLG serves as a natural carrier for various nutrients, such as vitamins and fatty acids.[23,24] Furthermore, BLG has demonstrated a significant resistance to peptic digestion[25] due to its compactly folded conformation originating from the abundance of rigid β-sheet structures,[26] while it is much more readily degraded by trypsin in the small intestine. These characteristics provide BLG-based delivery systems with desirable controlled release property. By far, various encapsulating systems have been developed with BLG, including emulsions,[27,28] nanoparticles,[29,30] and nanocomplexes.[31] These techniques have

Received: May 13, 2013
Revised: June 19, 2013

dx.doi.org/10.1021/bm4006886 | Biomacromolecules XXXX, XXX, XXX−XXX

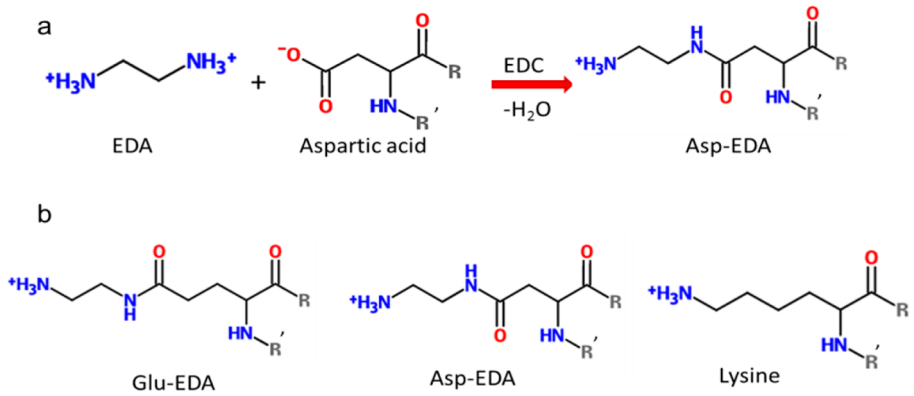

Figure 1. Illustration of the cationization procedure. (a) Theoretical equation for EDA-induced cationization. Both Asp and Glu residues were appropriate substrates. The net charge of each residue was altered by +2 (from −1 to +1) upon cationization. R and R′ were adjacent peptide chains. (b) Comparison of the EDA-Asp/EDA-Glu conjugate with lysine to display their geometric similarity.

demonstrated satisfactory protection to the entrapped compounds.

In this study, we are proposing a nanoparticle system prepared with cationic BLG (CBLG). We hypothesized that CBLG and CBLG-based delivery systems could inherit the merits of both a conventional cationic polymer and BLG, leading to a significant improvement in the encapsulation and absorption of bioactive compounds. It should be mentioned that a series of CBLGs were synthesized by Mattarella et al.[32] by amidation and esterification methods. However, their study was focused on functionality instead of encapsulation properties, and CBLGs prepared in that study might not be ideal for encapsulation due to their reduced solubility and increased digestibility.[32] To our knowledge, no study has been published so far on CBLG nanoparticles with an emphasis on encapsulation and delivery properties.

This paper was the first part of our study on CBLG nanoparticles. Ethylenediamine (EDA) was employed to synthesize CBLGs with sufficient positive charge and increased hydrophobicity, without compromising their original water solubility. The CBLGs were investigated for their physicochemical and conformational characteristics, which were then employed to explain their digestion-resistive and mucoadhesive properties. Finally, CBLG nanoparticles were prepared using a desolvation method, and its particle forming behavior was compared in parallel with BLG.

MATERIALS AND METHODS

Materials. The following chemicals were purchased from Sigma-Aldrich (St. Louis, MO, USA): bovine *β*-lactoglobulin (BLG, 90% purity), ethylenediamine dihydrochloride (EDA, 98% purity), *N*-(3-dimethylaminopropyl)-N-ethylcarbodiimide (EDC, 97% purity), 2,4,6-trinitrobenzenesulfonic acid (TNBS, 0.5 mg/mL water solution), 8-anilino-1-naphthalenesulfonic acid (ANS, 97% purity), pepsin (3200−4500 units/mg), trypsin (10 000 BAEE units/mg), papain (10 units/mg), trichloroacetic acid (TCA) and bovine serum albumin (BSA, 98% purity). Porcine stomach mucin (PSM, type III, contains 0.5−1.5% sialic acid) was obtained from Himedia Co., India. Hanks' balanced salt solution (HBSS, pH 7.4) and phosphate buffer saline (PBS, 100 mM, pH 7.4) were purchased from Invitrogen, Inc. (Carlsbad, CA, USA). All other reagents (sodium bicarbonate, acetone, acids and bases, etc.) were of analytical grade.

Preparation of CBLG. CBLG was prepared by grafting positively charged EDA moieties to the negatively charged carboxyl groups on the aspartic and glutamic acid residues (Figure 1). This was achieved via a carbodiimide-catalyzed approach that was previously reported.[33] In brief, 400 mg of BLG was dissolved in 5 mL deionized water, to which 50 mL of EDA solution at different concentrations (0.6, 0.9, 1.2, and 1.5 mol/L) was added under mild stirring. The mixture was adjusted to pH 4.75 with 1 mol/L HCl and equilibrated for 30 min. Cationization was initiated by the addition of 150 mg EDC and terminated by 540 *μ*L acetate buffer (4 mol/L, pH 4.75) after 2 h. The dispersion was dialyzed against deionized water at 4 °C for 48 h and freeze-dried. The moisture content of the final product was less than 5%, and the protein content was at least 90% according to a Bradford assay calibrated with BSA.

Determination of Primary Amino Group Contents and Net Charge. The contents of primary amino groups were determined by TNBS assay.[34] BLG and CBLG were dissolved in 0.1 mol/L $NaHCO_3$ buffer (pH 8.5) at a concentration of 100 *μ*g/mL, and 0.5 mL of 0.2 mg/mL TNBS solution was added to 1 mL of each sample. After incubation at 37 °C for 2 h, the dispersion was mixed with 0.5 mL 10% sodium dodecyl sulfate (SDS) solution and 0.25 mL 1 mol/L HCl to terminate the reaction. The resultant mixture was cooled to room temperature and measured for its absorbance at 420 nm using a DU-730 UV/vis spectrophotometer (Beckman Coulter Inc., Fullerton, CA, USA). A calibration curve (R^2 = 0.9997) was established following a similar procedure, except that a series of concentrations of BSA (59 primary amino groups per molecule from its lysine residues) was employed instead of BLG/CBLG. The primary amino group content was derived from the curve and then adopted to estimate the net charge of CBLG, considering that the introduction of each amino group altered the net charge of BLG by +2 (Figure 1). The change in molecular weight upon cationization was assumed negligible.

Determination of Zeta Potential. The dispersion of BLG or CBLG in PBS (10 mmol/L, pH 7.0, same hereinafter) and HBSS (140 mmol/L, no calcium or magnesium, pH 7.4, same hereinafter) was measured for its electrophoretic mobility by laser Doppler velocimetry using a Nano ZS90 Zetasizer (Malvern Inc., Malvern, UK). Each sample (1 mg/mL) was measured three times, and at least 12 runs were performed per measurement. The data were then converted to zeta potentials using the Smoluchowski model.

Determination of Surface Hydrophobicity. ANS fluorescence assay was carried out to determine the surface hydrophobicity of BLG and CBLG dispersions[35] in two buffers, i.e., PBS and HBSS. Stock solutions of proteins (BLG or CBLG, both at 1 mg/mL) and ANS (100 *μ*g/mL) were prepared in a same buffer and filtered through a 0.22 *μ*m Acrodisc syringe filter membrane (Pall Co., Newquay, UK). The resultant solutions were then mixed and diluted to achieve a fixed ANS concentration of 50 *μ*g/mL and a protein concentration ranging from 5 to 50 *μ*g/mL. After 1 h of incubation at 25 °C, the mixture was observed for its fluorescence intensity (FI) on a PerkinElmer Victor X3 multilabel plate reader (PerkinElmer Inc., Waltham, MA, USA). The excitation and emission wavelengths were 355 and 460 nm, respectively. For each protein sample, a linear regression equation was

dx.doi.org/10.1021/bm4006886 | *Biomacromolecules* XXXX, XXX, XXX−XXX

established for FI versus protein concentration ($R^2 > 0.995$), and the slope (S_o) was used as an index for surface hydrophobicity.

Secondary Structure Determination. Fourier-transform infrared (FT-IR) study was conducted to monitor the structural change of BLG upon cationization. The lyophilized samples (3 to 5 mg) were mounted onto a Jasco FT/IR 4100 spectrometer (Jasco Inc., Easton, MD, USA). The infrared transmittance was acquired at the wavenumbers from 1000 to 4000 cm^{-1} with a resolution of 2 cm^{-1}. At least 100 repeated scans were undertaken for each sample. The spectra were averaged, smoothed, corrected for their baselines and converted to absorbance with the Spectra Manager software (Jasco Inc., Easton, MD, USA).

For quantitative study, the IR spectra were further subjected to Fourier self-deconvolution (FSD) using the OMNIC software (Thermo Scientific, West Palm Beach, FL, USA). A bandwidth at half height of 23 cm^{-1} and an enhance factor (K value) of 2.7 was adopted over the wavenumbers ranging from 2000 to 1300 cm^{-1}, according to previous studies.[26,36] The FSD spectra were then curve fitted assuming a Gaussian band profile. The resolved peaks were validated only when they were also found on the inverted secondary derivative (ISD) spectra obtained over the same wavenumber range.[26] Peak assignment was carried out on the FSD spectra following literatures on native BLG,[26,36] and the content of each secondary structure was expressed as the percentage of area of the corresponding peaks.

Determination of in Vitro Digestibility. Two enzymes, pepsin, and trypsin, were employed to investigate the degradation of BLG and CBLG. For peptic digestion,[25] the samples and pepsin were dissolved separately at 1 mg/mL in 0.1 mol/L HCl, which was adjusted to pH 2.0 with 0.1 mol/L NaOH. For tryptic digestion, both the samples and trypsin were dispersed separately at the same concentrations in a $NaHCO_3$ buffer (0.1 mol/L, pH 8.0, same hereinafter). The dispersions were then preheated at 37 °C for 15 min. To 15 mL of protein solution, 75 μL of the enzyme solution was added, thus achieving a substrate-to-enzyme ratio of 200:1 (w/w). The resultant suspensions were incubated at 37 °C for preset times (from 10 min to 4 h), after which aliquots of 1.5 mL were drawn from the dispersions and mixed with 1.5 mL TCA solution (10% in water, w/v). The mixtures were allowed to stand at room temperature for 15 min and then centrifuged (9000*g*, 20 °C, 20 min). The precipitate was discarded, and the absorbance of the supernatant at 280 nm was recorded. For comparison purposes, a series of mixtures were prepared with BLG/CBLG and papain at a substrate-to-enzyme ratio of 20:1 (w/w) in a $NaHCO_3$ buffer. After 4 h of incubation at 37 °C, the hydrolysates were subjected to TCA precipitation, centrifugation, and spectrophotometric measurement as mentioned above. According to previous literature,[37] almost 100% of the BLG was degraded by papain within 2 h. Therefore, the absorbance at 280 nm of the supernatant after papain digestion was indicative for complete proteolysis, and the data obtained from all other treatments were divided by this value to provide an apparent digestibility.

Determination of Mucoadhesive Properties. *Turbidity Analysis.*[9] Samples (BLG or CBLG) and mucin (PSM) were dispersed at 10 and 1 mg/mL in PBS, respectively, and they were both passed through a 1.2 μm Acrodisc syringe filter. Thereafter, 4 mL of PSM dispersion was mixed with 0.1, 0.2, and 0.4 mL of protein solution in order to achieve protein concentrations of 0.25, 0.5, and 1 mg/mL, respectively. The mixture was then incubated at 37 °C for 1 h and cooled to room temperature. The absorbance of 400 nm was recorded, using pure PSM dispersion as the blank.

Quartz Crystal Microbalance (QCM) Analysis.[38] In the QCM study, two thin layers of PSM and protein were deposited sequentially onto a gold-coated AT-cut quartz crystal with a fundamental frequency of 4.95 MHz (QSX-301, Q-Sense Co., Linthicum, MD, USA), and the mass of deposited polymers was reflected by the change in frequency (Δf). Prior to the deposition, the crystal was soaked in Piranha solution ($NH_3{\cdot}H_2O{:}H_2O_2{:}H_2O$ = 1:1:5, v/v/v) for 15 min at 70 °C and dried with nitrogen. The crystal was then mounted on a Q-Sense E1 microbalance (Q-Sense Co., Linthicum, MD, USA), after which PBS was injected at a flow rate of 0.224 mL/min using a peristaltic pump (Ismatec Reglo, Glattbrugg, Switzerland). After the acquisition of a constant Δf, PSM solution (400 μg/mL in PBS, filtered through a 220 nm membrane) was introduced to the crystal chamber. This triggered a significant increase in Δf, which reached another plateau after approximately 10 min. A second rinse of PBS was applied to remove loosely bound PSM, after which the BLG/CBLG solution (1 mg/mL in PBS, passed through a 220 nm membrane) was injected to the chamber at the same flow rate. After 15 min of protein adsorption, the chamber was subjected to a final rinse of PBS, until the attainment of the third plateau of Δf. Changes in Δf, up to the 13th overtone, were collected by QTools 3 (Q-Sense Co., Linthicum, MD, USA). The fifth overtone was converted to deposited mass (in ng/cm^2 crystal surface) using the Sauerbrey model. Mucoadhesion was expressed as the mass ratio of BLG/CBLG to PSM deposited on the crystal surface.

Preparation of BLG/CBLG Nanoparticles. Nanoparticles were prepared with BLG/CBLG via a desolvation process.[29,39] Constant stirring (600 rpm) was applied throughout the mixing and cross-linking process. The protein was dissolved in deionized water at a preset concentration of 10 to 20 mg/mL (pH 7.5−8.0), and the dispersion was equilibrated for 1 h at room temperature. Thereafter, pure acetone was added dropwise to achieve an acetone/water ratio of 80/20 or 90/10 (v/v). The final protein concentration in the binary solvent was kept at 2 mg/mL. After 30 min of equilibration, glutaraldehyde was added as a cross-linker. The glutaraldehyde/protein mass ratio was set at 40 μg/mg in this study based on the lysine content of BLG (16 mol/mol), and it was adopted for all protein samples regardless of the extent of cationization. After 6 h of cross-linking, acetone was evaporated under a constant nitrogen flow and replaced with the same volume of deionized water. The resultant suspension containing the protein nanoparticles was stored at 4 °C for subsequent assays.

Determination of Particle Size and Count Rate. The particle size and count rate were determined[4] by dynamic laser scattering (DLS) using a BI-200 SM Goniometer Version 2 (Brookhaven Instrument Corp., Holtsville, New York, USA) equipped with a 35 mW He−Ne laser beam. All dispersions were measured without dilution. The following parameters were adopted: laser power of 10 mW, detection wavelength of 637 nm, scattering angle of 90°, temperature of 25 °C, and measurement time of 1 min. The refractive indices and viscosities of different acetone/water systems were applied for all assays, since they were not significantly altered by protein or glutaraldehyde in our study (data not shown). Two separate measurements were carried out to obtain accurate results. For count rate determination, the aperture pinhole size was fixed at 400 μm; to measure the particle size, appropriate aperture pinhole sizes were chosen to achieve a count rate between 100 and 300 kcps. The obtained data were analyzed using cumulant algorithm, and the quadratic mean particle size was reported.

Scanning Electron Microscopy (SEM). The morphology of BLG/CBLG nanoparticles was observed using a Hitachi SU-70 SEM (Hitachi, Pleasanton, CA, USA). Approximately 40 μL of the nanoparticle dispersions was dripped and cast-dried on an aluminum pan, which was cut into appropriate sizes and adhered to a 1-in. specimen stub with conductive carbon tapes (Electron Microscopy Sciences, Ft. Washington, PA, USA). To avoid the charging effect, a thin layer (<20 nm) of gold and platinum was deposited to the samples using a sputter coater (Hummer XP, Anatech, CA, USA) prior to the observation. Representative images were reported.

Statistics. All measurements were carried out in triplicates. The results were expressed as means ± standard error. For statistical analysis, the data were subjected to analysis of variance ($P < 0.05$) followed by Tukey's test with an experimentwise confidence level of α = 0.10, using SAS 9 software (SAS Institute Inc., Cary, NC, USA).

RESULT AND DISCUSSION

Change in Protein Net Charge upon Cationization. The numbers of amino and carboxyl groups of BLG and CBLG are compared in Supporting Information Table S1. The numbers in the sample names (0.6, 0.9, 1.2 and 1.5) indicate

dx.doi.org/10.1021/bm4006886 | Biomacromolecules XXXX, XXX, XXX−XXX

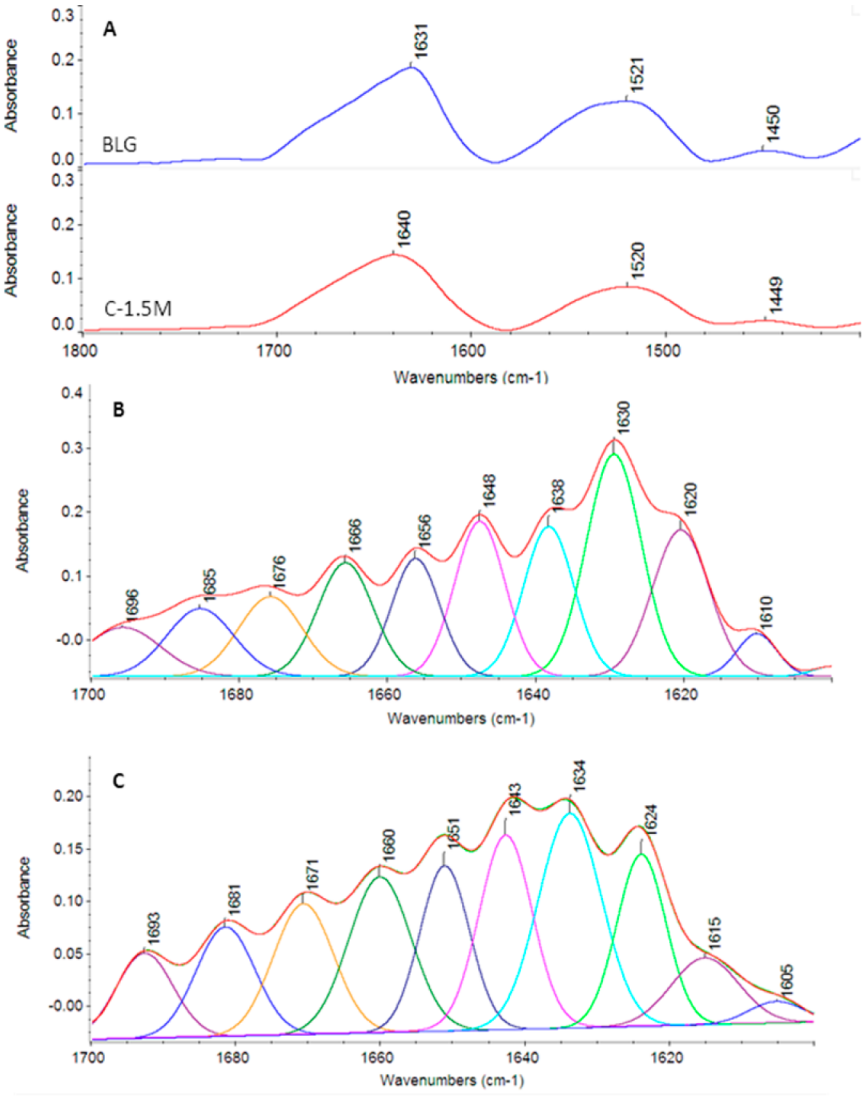

Figure 2. FT-IR spectra of BLG and C-1.5M. (A) Original spectra showing amide I, II, and III bands. (B,C) FSD and curve-fitted spectra depicting detailed secondary structure profiles of BLG (B) and C-1.5 M (C).

the molarity of EDA applied in the cationization process. A native BLG molecule possesses 16 lysine (TNBS-reactive), 3 arginine, 10 aspartic acid, and 16 glutamic acid residues,[40] all of which result in an overall charge of −7 per molecule. Our TNBS assay showed 16.3 reactive primary amino groups on BLG, which was consistent with the theoretical value. When an increasing amount of EDA was added during the cationization process, the number of primary amino groups increased progressively to a maximum of 27.3 per molecule. Meanwhile, the deduced number of total carboxyl groups was decreased from 25.7 to 13.7. These changes gave rise to a dramatic change in the net charge to +17 for C-1.2 M and C-1.5M. The relatively high density of positive charges possessed by CBLG may greatly benefit their mucoadhesive properties as well as cellular uptake, thus promoting the bioavailability of the bound nutraceuticals or drugs. It should be pointed out that cationic polymers may exhibit considerable cytotoxicity.[41,42] However, the toxicity of cationic protein was found to be the lowest among all cationic polymers,[43] probably owing to the biocompatibility of the original protein. The cytotoxicity of CBLG will be studied in our next study.

Surface Charge and Hydrophobicity. The impact of cationization on the surface charge and hydrophobicity of BLG is summarized in Table S2. The zeta potential of BLG in PBS was −37.0 mV, which was comparable with previously reported results.[44] As the degree of cationization increased, the zeta potential shifted significantly toward a more positive value. This phenomenon confirmed the shift in molecular net charges, and it was indicative for adequate exposure of the conjugated EDA moieties on the surface of the molecule. It was noteworthy that the zeta potentials of C-1.2 M (36.8 mV) and C-1.5 M (38.9 mV) were comparable in magnitude to that of native BLG (−37.0 mV). According to the American Society for Testing and Materials,[45] a zeta potential with an absolute value of higher than 30 mV is indicative for "moderate to good" stability of colloidal systems, due to the strong electrostatic repulsion between the charged molecules or particles. The satisfactory dispersion stability of CBLG was confirmed by our preliminary study (data not shown), in which CBLG was soluble in pure water or PBS at concentrations higher than 80 mg/mL.

BLG was reported to exhibit a relatively low surface hydrophobicity (S_o) in PBS of approximately 100.[44] This result was also confirmed by our study. The S_o of CBLG, on the other

dx.doi.org/10.1021/bm4006886 | Biomacromolecules XXXX, XXX, XXX−XXX

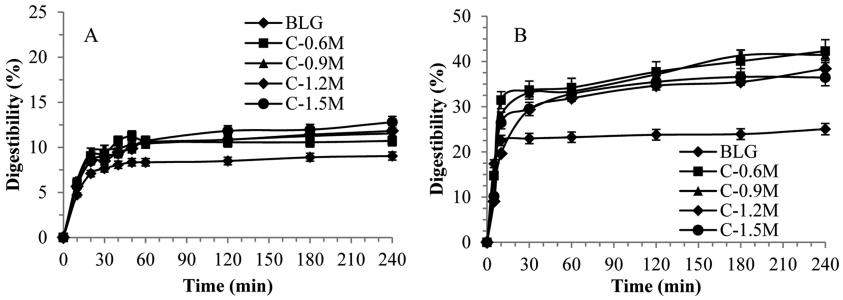

Figure 3. In vitro digestions of BLG and CBLG in the presence of (A) pepsin and (B) trypsin.

hand, was at most 1070% higher than that of BLG. In addition, the highest S_o achieved by CBLG (1270) was comparable with that of BSA (1000−2000),[46] a protein known for its high surface hydrophobicity. The remarkable increase in S_o by cationization was also observed on cationic BLG prepared by esterification and amidation,[32] and it was probably attributed to the following three reasons. First, the introduction and exposure of the hydrophobic backbones of EDA played a major role in increased protein−ANS hydrophobic binding, which yielded a higher S_o.[32] The positive charge on EDA, on the other hand, did not contribute significantly to the hydrophilicity or hydrophobicity of BLG, because it did not alter the magnitude of net charge on the Asp or Glu residue. Second, CBLG might have formed a certain amount of electrostatic complexes with the anionic ANS, which exhibited minor fluorescence.[47] Third, the randomization of BLG chain might have increased the quantum yield of ANS and led to an elevated apparent S_o.[48] This conformational change will be demonstrated in the next section. In addition to these three factors, enhanced protein aggregation upon cationization was also taken into consideration. However, no significant difference in turbidity was observed between BLG and CBLG solutions (data not shown). Therefore, this phenomenon was excluded from the possible reasons.

HBSS was selected as a second buffer for evaluating zeta potential and S_o, because of its resemblance to intracellular fluids. This buffer exhibited a similar pH (7.4) with the PBS used in our study (7.0), but it contained a 13-fold higher concentration of salt. As shown in Table S2, both BLG and CBLG exhibited decreased zeta potential (in terms of magnitude) and S_o, which was consistent with previous studies.[32,49] The reduced zeta potential was possibly attributed to the charge screening effect caused by increased ionic strength. Such change may result in weakened intra- and intermolecule electrostatic repulsions and, therefore, the adoption of more compact conformations by BLG/CBLG. Consequently, the exposure of the grafted hydrophobic EDA moieties might have been diminished in the presence of HBSS, and the surface hydrophobicity was hence decreased. In addition, the partial electrostatic complexation between protein and ANS might also have been compromised by charge screening, leading to a decrease in fluorescence intensity. In spite of these observations, the improvements in zeta potential and S_o by cationization were as remarkable in HBSS as were in PBS. These results suggested that CBLG might adhere to cell membrane more effectively through both electrostatic and hydrophobic interaction, thus enhancing the cellular uptake of the bound compounds of interest.

Secondary Structure. Protein conformation is a key factor that governs its physicochemical and functional properties. Conformational changes of protein have a significant influence on the hydrogen bonding intensity at the proximity of peptide bonds, altering their stretching patterns and consequentially changing the IR absorbance of the corresponding peaks, among which amide I (C═O stretching) exhibited the highest sensitivity.[50] As can be seen in Figure 2A, three characteristic peaks of native BLG were observed at 1631 (amide I, C═O stretching), 1521 (amide II, C−N stretching and N−H bending), and 1450 (amide III, CN stretching, NH bending) cm^{-1}. These observations were consistent with previous literature,[26] indicating the predominance of the β-sheet of BLG. After cationization, there was a significant shift of amide I to higher wavenumbers (1640 cm^{-1} for C-1.5M), while the shifts of amide II and III were not observed. This change suggested a decrease in the β-sheet component, together with an increase in α-helix or random coils.[51]

For quantitative assessment, the spectra were further subjected to FSD and Gaussian curve fitting procedure. Ten peaks were resolved and confirmed for both BLG and CBLG (Figure 2B,C), which were assigned to different secondary structure components according to previous studies.[26,36] As shown in Table S3, there was a significant increase in the percentages of α-helix (by 34%),[52] turns (by 33%)[53] and random coil (by 26%),[54] at the expense of β-sheet (decreased by 29%).[55] Such structural change was closely related to the consumption of glutamic acid and aspartic acid, both of which were found majorly in the β-sheet segments of BLG.[56] The conjugation of EDA moieties onto these amino acids might have weakened their ability to stabilize the relatively rigid β-sheet and produced flexible structures, such as helices, turns, and coils. Such conformational transformation suggested a less rigid and more randomized structure of CLBG compared to BLG, which was expected to have a positive impact on the encapsulation, transportation and delivery of nutraceuticals or drugs. These hypotheses will be tested in the follow-up study that will be focused on the incorporation, stabilization, and controlled release of nutrients and drugs.

Proteolysis Profiles. BLG is known for its resistance to peptic digestion,[25] a major advantage over other proteins with respect to the transportation and delivery of nutraceuticals and drugs. This character was confirmed by our study (Figure 3A), in which only 9% of BLG was degraded after 4 h of incubation with pepsin. As for CBLG, a similar resistance was also observed, although the percentage of digested protein increased slightly to 13%. This indigestibility of BLG by pepsin is attributed to the stability of the β-sheet-predominated structure.[25] In addition, pepsin preferably cleaves the peptide bonds formed between hydrophobic amino acids,[57] which are not sufficiently exposed as evidenced by a low surface hydrophobicity. As discussed in the previous section, a lower

dx.doi.org/10.1021/bm4006886 | Biomacromolecules XXXX, XXX, XXX−XXX

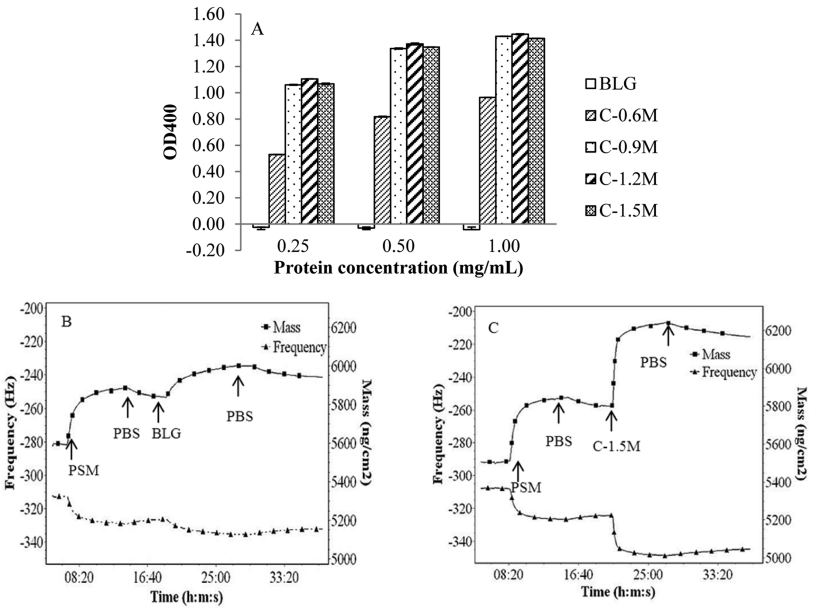

Figure 4. Mucoadhesive properties of BLG and CBLG. (A) Turbidity measurement at a PSM concentration of 1 mg/mL and different BLG/CBLG concentrations. (B,C) QCM analysis showing the mucoadhesion of BLG (B) and C-1.5 M (C), obtained at PSM and BLG/CBLG concentrations of 0.4 and 1 mg/mL, respectively. The fifth overtone was used for graph plotting and mass calculation.

content of β-sheet in CBLG might have resulted in decreased chain rigidity and increased flexibility compared to native BLG. However, the results from peptic digestion suggested that such change had only limited influence on the exposure of hydrophobic amino acid residues. In light of this result, it was speculated that the significant increase in S_o discussed before was more likely due to the exposure of EDA moieties than that of the original hydrophobic residues in BLG.

It was also noted that the Glu-/Asp-EDA conjugates produced upon cationization might be poor substrates for pepsin, in spite of the hydrophobicity caused by EDA. This was probably because these conjugates exhibited little geometric similarity to any naturally occurring hydrophobic amino acids. In addition, the positive charge on EDA might have inhibited the catalytic triad on pepsin from approaching its substrate. As a result, CBLG inherited the high resistance to peptic digestion from BLG, which may enable it to minimize the loss of the encapsulated nutraceuticals and drugs in the stomach.

Compared to pepsin, trypsin exhibited a higher capacity in digesting BLG, yielding an apparent digestibility of 25% (Figure 3) in the first 20 min. The abundance of positively charged amino acids (lysine and arginine) in BLG may account for this phenomenon, considering that they were typical substrates of trypsin.[32] As for CBLG, the EDA-aspartic acid conjugate carried as much positive charge as lysine, which showed a certain extent of geometric similarity to lysine as illustrated in Figure 1. These two characteristics, together with its sufficient exposure as discussed before, made EDA−aspartic acid conjugates a possible substrate for tryptic digestion. Consequentially, the apparent digestibility of CBLG was increased to at most 43% as expected. Similar results were reported previously for amidated and esterified BLG.[32]

Improved digestibility by trypsin may have two different impacts on the transportation and delivery of nutraceuticals or drugs. On one hand, it suggested a more complete degradation of the protein matrix, leading to a more complete release of the bound compound in small intestine. This property, together with the resistance to gastric digestion, is expected to confer CBLG nanoparticles with satisfactory controlled release feature. This hypothesis will be tested in our follow-up study. On the other hand, accelerated decomposition of the protein matrix in the digestive system implied weaker protection to the entrapped compounds in the circulation process. This disadvantage, however, could be overcome by choosing proper cationizing reagents. For example, polyethylenimine (PEI) carries an equally high density of positive charges as EDA, and it provides considerable steric hindrance to the protein due to its branched structure.[7] Cationization of BLG by PEI, therefore, is expected to detain both peptic and tryptic digestions, thus providing maximal protection to the incorporated compounds after intestinal absorption.

Mucoadhesive Properties. The gel-like layer of mucin on the wall of the small intestine serves as the first barrier for nutrient absorption.[58] The adhesion to this negative charged, highly glycosylated protein is vital for the diffusion and transportation of enteric nutraceuticals or drugs, and it is one of the key components of the rationale of protein cationization. Two methods, turbidity and QCM assay, were employed in this study to validate the improved mucoadhesion of CBLG. In the turbidity analysis (Figure 4A), a BLG−PSM mixture exhibited a negative absorbance at both 400 and 500 nm (the latter is not shown), regardless of the concentration of BLG. This result was probably due to the negative net charges on both BLG and PSM, which inhibited the association between these two molecules through a strong electrostatic repulsion. On the contrary, the dispersions containing CBLG and PSM exhibited a highly positive absorbance. The relatively low absorbance of C-0.6 M compared to other CBLGs was probably attributed to its lower surface charge as discussed before. These phenomena suggested the extensive formation of CBLG-PSM aggregates, which might have been driven by electrostatic attraction and, less importantly, hydrophobic interaction.

The enhanced mucoadhesion property of CBLG was also evidenced by QCM analysis. Figure 4B,C were typical QCM diagrams obtained with PSM-BLG and PSM-CBLG, respectively. The two stepwise increases in the adsorbed mass

dx.doi.org/10.1021/bm4006886 | Biomacromolecules XXXX, XXX, XXX−XXX

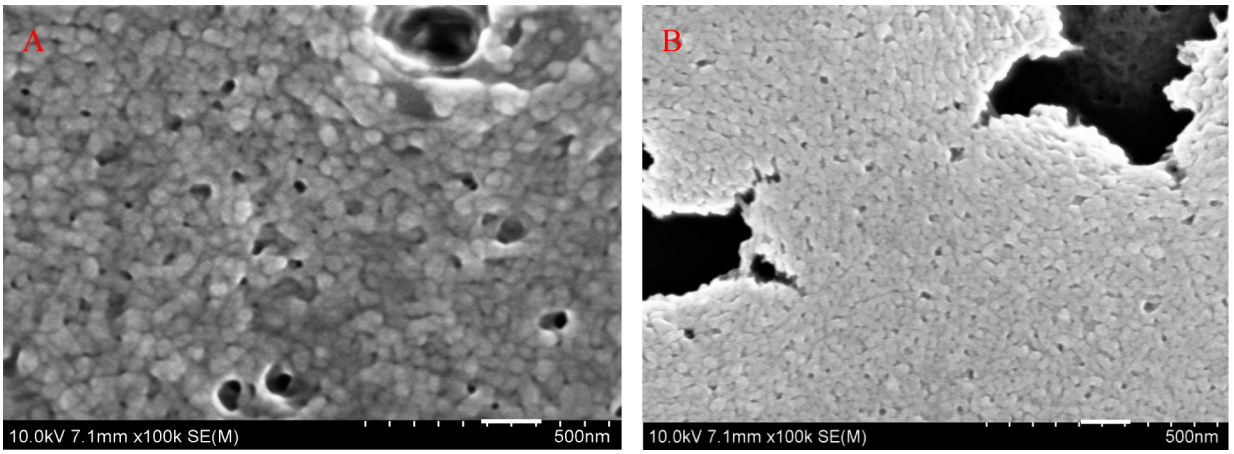

Figure 5. SEM images for nanoparticles formed by BLG (A) and C-1.5 M (B). The white scale bar indicates 100 nm. Images were taken after acetone was evaporated and replaced with same volume of deionized water.

corresponded sequentially to the deposition of PSM onto the gold crystal and the adsorption of BLG/CBLG onto the PSM layer. Compared with BLG, CBLG adsorbed to PSM at a significantly higher level. Furthermore, the adsorption of CBLG reached equilibrium within a shorter time, as suggested by a steeper slope of the second step. A quantitative comparison in the mucoadhesive properties is displayed in Table S4 based on QCM analysis. The mass ratio of adsorbed protein to that of PSM increased in parallel with the cationization degrees and reached a maximum of 1.259 (C-1.5M), which is 252% higher than that corresponding to BLG (0.357). It was worth mentioning that a certain amount of BLG adsorbed to PSM in the QCM study, which was not observed in turbidity analysis. A possible explanation for this discrepancy was that part of the hydrophilic oligosaccharide chains that originally covered the protein segment of PSM[58] might have been reorientated to facilitate its deposition on the gold crystal. Such a process facilitated the exposure of the more hydrophobic protein moieties,[58] enabling them to associate with BLG through hydrophobic interaction.

Elevated mucoadhesive property of CBLG is one of its major merits. It resulted in shorter dwelling time in the small intestine, which suggests reduced opportunity for protein digestion and nutrient degradation. Both of these factors facilitated the absorption of CBLG and CBLG-bound molecules in their intact form. Although a number of studies have shown comparable mucoadhesion of other cationic polymers,[9,38,59] most of them were conducted under acidic conditions (pH 2−6). This was possibly due to the low solubility at neutral or basic pH of these polymers. Such disadvantage would have a negative impact on the mucoadhesive capability in small intestine, whose average pH is around 7. CBLG, on the other hand, exhibited high solubility at neutral pH due to its amphiphilic nature. Such advantage made CBLG a suitable candidate for the transportation of nutraceuticals and drugs across the small intestine.

Particle Formation Behaviors. The particle forming properties of BLG and CBLG investigated by DLS are compared in Table S5. In our preliminary study (data not shown), both BLG and C-0.6 M aggregated spontaneously into nanoparticles in the presence of 80% aqueous ethanol. The other CBLGs (C-0.9M, C-1.2 M and C-1.5M), however, did not show any observable aggregation even in 95% ethanol. Acetone, on the other hand, was able to initiate the particle formation of BLG and all CBLGs. It is generally believed that the formation of protein nanoparticles begins with the exposure of functional groups (hydrophobic site, thiol group, etc.), which induced intermolecular association and particle formation.[29,39] Such process requires the contact between protein and antisolvent molecules, which triggers the unfolding of peptide chains.[60] When BLG was cationized, a considerable part of its exterior was covered by the grafted EDA moieties, as indicated by the highly positive zeta potential. Such coverage produced extra hindrance for relative polar organic solvents such as ethanol, due to the size of the cationizer (EDA) and the increase in surface hydrophobicity it induced.[61] This explained why ethanol desolvated BLG and C-0.6 M effectively but did not work for CBLGs with higher cationization degrees. In addition, C-0.6 M might have exhibited weaker electrostatic repulsion due to a lower surface charge, which also facilitated the aggregation. As for acetone, it possessed a stronger protein denaturation capacity than ethanol.[60] In addition, its relatively low polarity suggested better contact with the hydrophobic surface of CBLG,[62] which further promoted the desolvation and protein unfolding processes.

As shown in Table S5, the particles formed with BLG or CBLG exhibited an average size of 75−172 nm, which was ideal for the encapsulation and transportation of nutraceuticals and drugs.[63] In addition, all samples except C-0.6 M exhibited lower particle size, higher count rate and lower polydispersity in 90% acetone as compared to 80% acetone. The count rate of a colloidal dispersion is proportional to the quantity of particles and the sixth power of the average size; therefore, these results suggested that a significantly greater number of nanoparticles with smaller, more uniformly distributed size were formed in 90% acetone. The precipitation of C-0.6 M in 90% acetone was probably due to the lack of electrostatic stabilization as discussed before.

Figure 5 displayed the morphology of BLG (A) and CBLG (B) nanoparticles observed under SEM. The particles were approximately spherical, and they exhibited a narrow size distribution between 50 and 80 nm. The maintenance of particle structure after the evaporation of acetone evidenced successful cross-linking of the particle structure by glutaraldehyde. The fact that the sizes observed under SEM were lower than those obtained by DLS was probably due to the shrinkage of nanoparticles under vacuum. Similar results were reported previously.[2,64]

dx.doi.org/10.1021/bm4006886 | *Biomacromolecules* XXXX, XXX, XXX−XXX

CONCLUSIONS

CBLG, a highly water-soluble cationic protein, was synthesized successfully with BLG and EDA. The attachment of EDA moieties induced a reversal in zeta potential (from −37 to +39 mV), together with a significant increase in surface hydrophobicity. FT-IR study showed the increase in helical and random secondary structure upon cationization at the expense of rigid β-sheets. Such conformational change led to an increase of apparent digestibility by trypsin, whereas the original resistance to peptic digestion of BLG was maximally retained. With regard to absorption, CBLG exhibited significantly enhanced association with PSM in turbidity assay compared with BLG, and its adsorption to PSM layer was improved by up to 252% in the QCM study. Nanoparticles with sub-100 nm size and narrow size distribution were prepared with CBLG using acetone as an antisolvent, evidenced by DLS and SEM. These features made CBLG and CBLG-based nanoparticles a suitable candidate for the encapsulation and delivery of poorly bioavailable nutraceuticals or drugs. Follow-up studies are being carried out on CBLG nanoparticles to evaluate their encapsulation capacity, controlled release in simulated GI tract, as well as their toxicological properties.

ASSOCIATED CONTENT

Supporting Information

The following information on BLG and CBLG is provided in Tables S1−S5: amino group contents and net charges, zeta potential and hydrophobicity in PBS and HBSS, peak assignment and percentage of secondary structure patterns, quantitative comparison in mucoadhesive properties, and characterization of nanoparticles. This material is available free of charge via the Internet at http://pubs.acs.org.

AUTHOR INFORMATION

Corresponding Author

*Tel: (301)-405-8421; Fax: (301)-314-3313; E-mail: wangqin@umd.edu.

Notes

The authors declare no competing financial interest.

ACKNOWLEDGMENTS

The authors are grateful for the technical support of the NanoCenter of the University of Maryland in scanning electron microscopy.

REFERENCES

(1) Kawashima, Y. Nanoparticulate systems for improved drug delivery. *Adv. Drug Delivery Rev.* **2001**, *47*, 1−2.

(2) Luo, Y.; Teng, Z.; Wang, Q. Development of zein nanoparticles coated with carboxymethyl chitosan for encapsulation and controlled release of vitamin D3. *J. Agric. Food. Chem.* **2012**, *60*, 836−843.

(3) Andrews, G. P.; Jones, D. S. Rheological characterization of bioadhesive binary polymeric systems designed as platforms for drug delivery implants. *Biomacromolecules* **2006**, *7*, 899−906.

(4) Teng, Z.; Luo, Y.; Wang, T.; Zhang, B.; Wang, Q. Development and application of nanoparticles synthesized with folic acid conjugated soy protein. *J. Agric. Food. Chem.* **2013**, *61*, 2556−2564.

(5) Delgado, C.; Francis, G. E.; Fisher, D. The uses and properties of PEG-Linked Proteins. *Crit. Rev. Ther. Drug Carrier Syst.* **1992**, *9*, 249−304.

(6) Chen, L.; Remondetto, G. E.; Subirade, M. Food protein-based materials as nutraceutical delivery systems. *Trends Food Sci. Technol.* **2006**, *17*, 272−283.

(7) Futami, J.; Kitazoe, M.; Murata, H.; Yamada, H. Exploiting protein cationization techniques in future drug development. *Expert Opin. Drug Discovery* **2007**, *2*, 261−269.

(8) Liu, X. F.; Zhi, X. N.; Liu, Y. F.; Wu, B.; Sun, Z.; Shen, J. Effect of chitosan, O-carboxymethyl chitosan, and *N*-[(2-hydroxy-3-*N*,*N*-dimethylhexadecyl ammonium)propyl] chitosan chloride on overweight and insulin resistance in a murine diet-induced obesity. *J. Agric. Food. Chem.* **2012**, *60*, 3471−3476.

(9) Thongborisute, J.; Takeuchi, H. Evaluation of mucoadhesiveness of polymers by BIACORE method and mucin-particle method. *Int. J. Pharm.* **2008**, *354*, 204−209.

(10) Bengoechea, C.; Jones, O. G.; Guerrero, A.; McClements, D. J. Formation and characterization of lactoferrin/pectin electrostatic complexes: Impact of composition, pH and thermal treatment. *Food Hydrocolloids* **2011**, *25*, 1227−1232.

(11) Bengoechea, C.; Peinado, I.; McClements, D. J. Formation of protein nanoparticles by controlled heat treatment of lactoferrin: Factors affecting particle characteristics. *Food Hydrocolloids* **2011**, *25*, 1354−1360.

(12) Tang, H. Y.; Yin, L. C.; Lu, H.; Cheng, J. J. Water-soluble poly(L-serine)s with elongated and charged side-chains: Synthesis, conformations, and cell-penetrating properties. *Biomacromolecules* **2012**, *13*, 2609−2615.

(13) Shen, W.-C.; Ryser, H. Conjugation of poly-L-lysine to albumin and horseradish peroxidase: A novel method of enhancing the cellular uptake of proteins. *Proc. Natl. Acad. Sci. U.S.A.* **1978**, *75*, 1872−1876.

(14) Kim, S. H.; Jeong, J. H.; Chun, K. W.; Park, T. G. Target-specific cellular uptake of PLGA nanoparticles coated with poly(L-lysine)−poly(ethylene glycol)−folate conjugate. *Langmuir* **2005**, *21*, 8852−8857.

(15) Watkins, C. L.; Brennan, P.; Fegan, C.; Takayama, K.; Nakase, I.; Futaki, S.; Jones, A. T. Cellular uptake, distribution and cytotoxicity of the hydrophobic cell penetrating peptide sequence PFVYLI linked to the proapoptotic domain peptide PAD. *J. Controlled Release* **2009**, *140*, 237−44.

(16) Lindgren, M.; Hällbrink, M.; Prochiantz, A.; Langel, Ü. Cell-penetrating peptides. *Trends Pharmacol. Sci.* **2000**, *21*, 99−103.

(17) Deshayes, S.; Morris, M.; Divita, G.; Heitz, F. Cell-penetrating peptides: Tools for intracellular delivery of therapeutics. *Cell. Mol. Life Sci.* **2005**, *62*, 1839−1849.

(18) Lim, Y.-b.; Lee, E.; Lee, M. Cell penetrating peptide-coated nanoribbons for intracellular nanocarriers. *Angew. Chem.* **2007**, *119*, 3545−3548.

(19) Hu, B.; Wang, S. S.; Li, J.; Zeng, X. X.; Huang, Q. R. Assembly of bioactive peptide−chitosan nanocomplexes. *J. Phys. Chem. B* **2011**, *115*, 7515−7523.

(20) Qi, L. F.; Wu, L. X.; Zheng, S.; Wang, Y. L.; Fu, H. L.; Cui, D. X. Cell-penetrating magnetic nanoparticles for highly efficient delivery and intracellular imaging of siRNA. *Biomacromolecules* **2012**, *13*, 2723−2730.

(21) Furlund, C. B.; Kristoffersen, A. B.; Devold, T. G.; Vegarud, G. E.; Jonassen, C. M. Bovine lactoferrin digested with human gastrointestinal enzymes inhibits replication of human echovirus 5 in cell culture. *Nutr. Res. (N.Y.)* **2012**, *32*, 503−513.

(22) Jones, O. G.; Handschin, S.; Adamcik, J.; Harnau, L.; Bolisetty, S.; Mezzenga, R. Complexation of β-lactoglobulin fibrils and sulfated polysaccharides. *Biomacromolecules* **2011**, *12*, 3056−3065.

(23) Papiz, M.; Sawyer, L.; Eliopoulos, E.; North, A.; Findlay, J.; Sivaprasadarao, R.; Jones, T.; Newcomer, M.; Kraulis, P. The structure of β-lactoglobulin and its similarity to plasma retinol-binding protein. *Nature* **1986**, *324*, 383−385.

(24) Kontopidis, G.; Holt, C.; Sawyer, L. Invited review: β-Lactoglobulin: binding properties, structure, and function. *J. Dairy Sci.* **2004**, *87*, 785−796.

(25) Reddy, I. M.; Kella, N. K. D.; Kinsella, J. E. Structural and conformational basis of the resistance of β-lactoglobulin to peptic and chymotryptic digestion. *J. Agric. Food. Chem.* **1988**, *36*, 737−741.

(26) Dong, A.; Matsuura, J.; Allison, S. D.; Chrisman, E.; Manning, M. C.; Carpenter, J. F. Infrared and circular dichroism spectroscopic

characterization of structural differences between β-lactoglobulin A and B. *Biochemistry* **1996**, *35*, 1450−1457.
(27) Given, P. S., Jr Encapsulation of flavors in emulsions for beverages. *Curr. Opin. Colloid Interface Sci.* **2009**, *14*, 43−47.
(28) Zhang, W.; Zhong, Q. Microemulsions as nanoreactors to produce whey protein nanoparticles with enhanced heat stability by thermal pretreatment. *Food Chem.* **2010**, *119*, 1318−1325.
(29) Ko, S.; Gunasekaran, S. Preparation of sub-100-nm β-lactoglobulin (BLG) nanoparticles. *J. Microencapsul.* **2006**, *23*, 887−98.
(30) Chen, L.; Subirade, M. Chitosan/β-lactoglobulin core-shell nanoparticles as nutraceutical carriers. *Biomaterials* **2005**, *26*, 6041−6053.
(31) Zimet, P.; Livney, Y. D. Beta-lactoglobulin and its nanocomplexes with pectin as vehicles for ω-3 polyunsaturated fatty acids. *Food Hydrocolloids* **2009**, *23*, 1120−1126.
(32) Mattarella, N. L.; Richardson, T. Physicochemical and functional properties of positively charged derivatives of bovine β-lactoglobulin. *J. Agric. Food. Chem.* **1983**, *31*, 972−978.
(33) Hoare, D. G.; Koshland, D. E. A method for quantitative modification and estimation of carboxylic acid groups in proteins. *J. Biol. Chem.* **1967**, *242*, 2447.
(34) Castaneda, L.; Valle, J.; Yang, N.; Pluskat, S.; Slowinska, K. Collagen cross-linking with Au nanoparticles. *Biomacromolecules* **2008**, *9*, 3383−3388.
(35) Laligant, A.; Dumay, E.; Valencia, C. C.; Cuq, J. L.; Cheftel, J. C. Surface hydrophobicity and aggregation of β-lactoglobulin heated near neutral pH. *J. Agric. Food. Chem.* **1991**, *39*, 2147−2155.
(36) Bhattacharjee, C.; Saha, S.; Biswas, A.; Kundu, M.; Ghosh, L.; Das, K. P. Structural changes of β-lactoglobulin during thermal unfolding and refolding - An FT-IR and circular dichroism study. *Protein J.* **2005**, *24*, 27−35.
(37) Otte, J.; Zakora, M.; Qvist, K. B.; Olsen, C. E.; Barkholt, V. Hydrolysis of bovine β-lactoglobulin by various proteases and identification of selected peptides. *Int. Dairy J.* **1997**, *7*, 835−848.
(38) Wiecinski, P. N.; Metz, K. M.; Mangham, A. N.; Jacobson, K. H.; Hamers, R. J.; Pedersen, J. A. Gastrointestinal biodurability of engineered nanoparticles: Development of an in vitro assay. *Nanotoxicology* **2009**, *3*, 202−214.
(39) Teng, Z.; Luo, Y. C.; Wang, Q. Nanoparticles synthesized from soy protein: Preparation, characterization, and application for nutraceutical encapsulation. *J. Agric. Food. Chem.* **2012**, *60*, 2712−2720.
(40) Stein, W. H. Amino acid composition of β-lactoglobulin and bovine serum albumin. *J. Biol. Chem.* **1949**, *178*, 79−91.
(41) Stasko, N. A.; Johnson, C. B.; Schoenfisch, M. H.; Johnson, T. A.; Holmuhamedov, E. L. Cytotoxicity of polypropylenimine dendrimer conjugates on cultured endothelial cells. *Biomacromolecules* **2007**, *8*, 3853−3859.
(42) Hu, B.; Ting, Y.; Zeng, X.; Huang, Q. Cellular uptake and cytotoxicity of chitosan−caseinophosphopeptides nanocomplexes loaded with epigallocatechin gallate. *Carbohydr. Polym.* **2012**, *89*, 362−370.
(43) Fischer, D.; Li, Y.; Ahlemeyer, B.; Krieglstein, J.; Kissel, T. In vitro cytotoxicity testing of polycations: Influence of polymer structure on cell viability and hemolysis. *Biomaterials* **2003**, *24*, 1121−1131.
(44) Laligant, A.; Dumay, E.; Casas Valencia, C.; Cuq, J. L.; Cheftel, J. C. Surface hydrophobicity and aggregation of β-lactoglobulin heated near neutral pH. *J. Agric. Food. Chem.* **1991**, *39*, 2147−2155.
(45) Zeta Potential of Colloids in Water and Waste Water. In *ASTM Standard D*; American Society for Testing and Materials: West Conshohocken, PA, 1985; pp 4187−82.
(46) Cardamone, M.; Puri, N. K. Spectrofluorimetric assessment of the surface hydrophobicity of proteins. *Biochem. J.* **1992**, *282* (Pt 2), 589−93.
(47) Gasymov, O. K.; Glasgow, B. J. ANS fluorescence: Potential to augment the identification of the external binding sites of proteins. *Biochim. Biophys. Acta: Proteins Proteomics* **2007**, *1774*, 403−411.
(48) Penzer, G. R. 1-Anilinonaphthalene-8-sulphonate. *Eur. J. Biochem.* **1972**, *25*, 218−228.
(49) Tcholakova, S.; Denkov, N. D.; Sidzhakova, D.; Ivanov, I. B.; Campbell, B. Effects of electrolyte concentration and pH on the coalescence stability of β-lactoglobulin emulsions: Experiment and interpretation. *Langmuir* **2005**, *21*, 4842−4855.
(50) Kong, J.; Yu, S. Fourier transform infrared spectroscopic analysis of protein secondary structures. *Acta Biochim. Biophys. Sin.* **2007**, *39*, 549−559.
(51) Carbonaro, M.; Nucara, A. Secondary structure of food proteins by Fourier transform spectroscopy in the mid-infrared region. *Amino Acids* **2010**, *38*, 679−690.
(52) Surewicz, W. K.; Mantsch, H. H.; Chapman, D. Determination of protein secondary structure by Fourier transform infrared spectroscopy: A critical assessment. *Biochemistry* **1993**, *32*, 389−394.
(53) Zhang, J.; Liang, L.; Tian, Z.; Chen, L.; Subirade, M. Preparation and *in vitro* evaluation of calcium-induced soy protein isolate nanoparticles and their formation mechanism study. *Food Chem.* **2012**, *133*, 390−399.
(54) Byler, D. M.; Susi, H. Examination of the secondary structure of proteins by deconvolved FTIR spectra. *Biopolymers* **1986**, *25*, 469−487.
(55) Dong, A.; Huang, P.; Caughey, W. S. Protein secondary structures in water from second-derivative amide I infrared spectra. *Biochemistry* **1990**, *29*, 3303−3308.
(56) Alexander, L. J.; Hayes, G.; Pearse, M. J.; Beattie, C. W.; Stewart, A. F.; Willis, I. M.; Mackinlay, A. G. Complete sequence of the bovine β-lactoglobulin cDNA. *Nucleic Acids Res.* **1989**, *17*, 6739.
(57) Hedstrom, L. Serine protease mechanism and specificity. *Chem. Rev.* **2002**, *102*, 4501−4524.
(58) Bansil, R.; Turner, B. S. Mucin structure, aggregation, physiological functions and biomedical applications. *Curr. Opin. Colloid Interface Sci.* **2006**, *11*, 164−170.
(59) Sogias, I. A.; Williams, A. C.; Khutoryanskiy, V. V. Why is chitosan mucoadhesive? *Biomacromolecules* **2008**, *9*, 1837−1842.
(60) Khmelnitsky, Y. L.; Mozhaev, V. V.; Belova, A. B.; Sergeeva, M. V.; Martinek, K. Denaturation capacity: A new quantitative criterion for selection of organic solvents as reaction media in biocatalysis. *Eur. J. Biochem.* **1991**, *198*, 31−41.
(61) Mattarella, N. L.; Richardson, T. Physicochemical and functional properties of positively charged derivatives of bovine β-lactoglobulin. *J. Agric. Food Chem.* **1983**, *31*, 972−978.
(62) Teng, Z.; Wang, Q. Extraction, identification and characterization of the water-insoluble proteins from tobacco biomass. *J. Sci. Food Agric.* **2012**, *92*, 1368−1374.
(63) MaHam, A.; Tang, Z. W.; Wu, H.; Wang, J.; Lin, Y. H. Protein-based nanomedicine platforms for drug delivery. *Small* **2009**, *5*, 1706−1721.
(64) Luo, Y.; Wang, T.; Teng, Z.; Chen, P.; Sun, J.; Wang, Q. Encapsulation of indole-3-carbinol and 3,3′-diindolylmethane in zein/carboxymethyl chitosan nanoparticles with controlled release property and improved stability. *Food Chem.* **2013**, *139*, 224−230.